



RESEARCH ARTICLE

EFFECTS of LOW REACTION RATE on ZNO THIN FILMS PRODUCED by a CHEMICAL BATH DEPOSITION METHOD

Metehan ÖNAL^{1*}, Barış ALTIOKKA²

¹Bilecik Şeyh Edebalı University, Vocational School, Bilecik, metehan.onal@bilecik.edu.tr,
ORCID:0000-0001-7128-7123

²Bilecik Şeyh Edebalı University, Vocational School, Bilecik, baris.altiokka@bilecik.edu.tr,
ORCID0000-0001-8891-973X

Receive Date:03.06.2022

Accepted Date: 24.06.2022

ABSTRACT

In the presented study, while ZnO thin films were deposited onto glass substrates, chemical bath deposition method was used and Na₂S₂O₃ was used as an inhibitor to reduce the reaction rate. Four different samples were produced using 0, 4, 8 and 16mM Na₂S₂O₃, respectively. The images obtained from the scanning electron microscope showed that the amount of nano flowers on the film surfaces decreased due to the increase in the amount of inhibitor. The X-ray diffraction results were consistent with the ASTM card and showed that all the films were crystallized in a hexagonal structure. UV measurements showed that the absorbance value of the sample obtained without the use of inhibitor was up to four times higher than the other samples. It was observed that the energy band gaps of the films increased up to 4.24 eV depending on the amount of inhibitor. Visual analysis showed that all films adhered very well to the glass surface.

Keywords: ZnO, Thin film, Chemical bath deposition, Inhibitor

1. INTRODUCTION

Thin films, which have an important place for scientific and industrial studies due to their wide application areas, attract the attention of researchers, while zinc oxide (ZnO) thin films get their share of this interest. Zinc oxide is a non-toxic, low-cost and easily accessible [1]. Showing n-type semiconductor properties due to the presence of oxygen vacancies, ZnO has an energy band gap of 3.37 eV and an exciton binding energy of 60 meV at room temperature [2–4]. Application areas of ZnO thin films include many applications such as optoelectronic devices, photo-catalysts, and ultraviolet laser diodes, cathode ray tubes, gas sensors and piezoelectric transducers [5–8]. ZnO thin films are used as conductive and optical cover layers of large-area solar cells [9].

ZnO crystallizes in a hexagonal wurtzite structure [10, 11]. Many techniques are used to produce zinc oxide thin films. These techniques include magnetron sputtering, electro deposition, pulsed laser deposition (PLD), thermal oxidation, spray pyrolysis, chemical vapor deposition (CVD), sol-gel techniques, and chemical bath deposition (CBD) [12–18]. In the present study, the chemical bath deposition technique was chosen to deposit ZnO thin films due to its advantages such as simplicity of the required equipment, ability to be deposited at relatively low temperatures, and low cost.

While producing compound semiconductors with CBD, many properties that can be changed and controlled such as solution temperature, mixing speed, pH value, complex agent type and amount, deposition time have been investigated by researchers [8, 9, 19, 20]. However, no study was found in which Sodium thiosulfate ($\text{Na}_2\text{S}_2\text{O}_3$) was used as an inhibitor in the precipitation of ZnO thin films. In addition, in a study, it was reported that the reaction rate was reduced by using Sodium sulfite (Na_2SO_3) while producing ZnO thin films. In that study, the use of inhibitor significantly affected the crystallite dimensions and increased the energy band gaps 1.03V more than the previous value [21].

In this study, the reaction rate was reduced by using $\text{Na}_2\text{S}_2\text{O}_3$ in three different molarities as inhibitor. $\text{Na}_2\text{S}_2\text{O}_3$ was used for the first time in the literature for ZnO precipitation by chemical bath deposition method. It has been observed that the absorbance values of the films produced by using inhibitor during ZnO production were quite low, and in parallel with this, their transmittance values were quite high. The energy band gap values of the films were 3.89 eV when no inhibitor was used. When the inhibitor was used, it ranged from 4.13 eV to 4.24 eV. Analyzes using SEM images magnified 1000 times and 20000 times showed that as the amount of $\text{Na}_2\text{S}_2\text{O}_3$ increased, the nano-flowers on the film surfaces decreased.

2. EXPERIMENTAL DETAILS

ZnO thin films were deposited on glass substrates using the chemical bath deposition method. Before starting the deposition process, glass substrates were washed with acetone and rinsed with deionized water. While the first sample labeled S0 was produced, 60 mM ZnCl_2 and 8 mM EDTA were dissolved in 100 ml of deionized water without using an inhibitor, and ammonia (NH_3) was added with a dropper until the pH value of the solution was 9.5. While producing the samples labeled S1, S2 and S3, 4, 8 and 16 mM $\text{Na}_2\text{S}_2\text{O}_3$ were added to the final solution, respectively. While all samples were being fabricated, the solution temperature was kept at 85 ± 2 °C and mixed at 600 rpm. The deposition process was continued for 20, 25, 30 and 35 minutes, respectively, depending on the amount of inhibitor. When the deposition process was completed, the films were rinsed by using deionized water, labeled and left to dry at room conditions. Experimental conditions were tabulated and given in Table 1.

Table 1. Experimental conditions for ZnO deposited by chemical bath deposition method.

Experiments	ZnCl ₂ (mM)	EDTA (mM)	Temp. (°C)	Ph	Na ₂ S ₂ O ₃ (mM)	Deposition time (min)
S0	60	8	85±2	9.5	0	20
S1	60	8	85±2	9.5	4	25
S2	60	8	85±2	9.5	8	30
S3	60	8	85±2	9.5	16	35

The thickness of ZnO thin films was calculated using the Gravimetric method which has been given in Eq. 1 [22].

$$t = \frac{m}{\rho A} \quad (1)$$

In this equation, t is the film thickness, m is the mass of the film, ρ is the density, and A is the surface area. The bulk density value for ZnO is 5.675 g/cm^3 [23].

The thickness of the films named S0 and S1 was calculated as 480 nm on average. Moreover, the thickness of the sample named S2 was approximately 400 nm, and the thickness of S3 was approximately 380 nm. These results showed that the thickness of the produced samples decreased as the amount of $\text{Na}_2\text{S}_2\text{O}_3$ used increased.

A PANalytic Empyrean XRD was used to perform structural analyzes of ZnO films, a AandE lab with single-beam UV-vis spectrometer and a Zeiss SUPRA 40VP SEM to determine their optical and morphological properties, respectively.

3. RESULT AND DISCUSSION

3.1. Structural analysis of ZnO Films

In Figure 1, XRD diffraction patterns are given for ZnO thin films obtained depending on the amount of $\text{Na}_2\text{S}_2\text{O}_3$ added to the solution. When Figure 1 was examined, it was seen that all the films were formed in a hexagonal structure and all of the matched the ASTM card no 98-005-7478. Preferred orientations of the films were determined by using the TC (Texture coefficient) given in Eq. 2. [24].

$$TC = \frac{I_{(hkl)}/I_{0(hkl)}}{\frac{1}{N} \sum_N \left(\frac{I_{(hkl)}}{I_{0(hkl)}} \right)} \quad (2)$$

Table1. Calculated Texture Coefficients of ZnO films.

Experiments	S0	S1	S2	S3
T.C.(010)	0.92	0.95	0.85	0.85
T.C.(002)	0.68	0.79	0.85	1.00
T.C.(011)	1.39	1.25	1.30	1.25

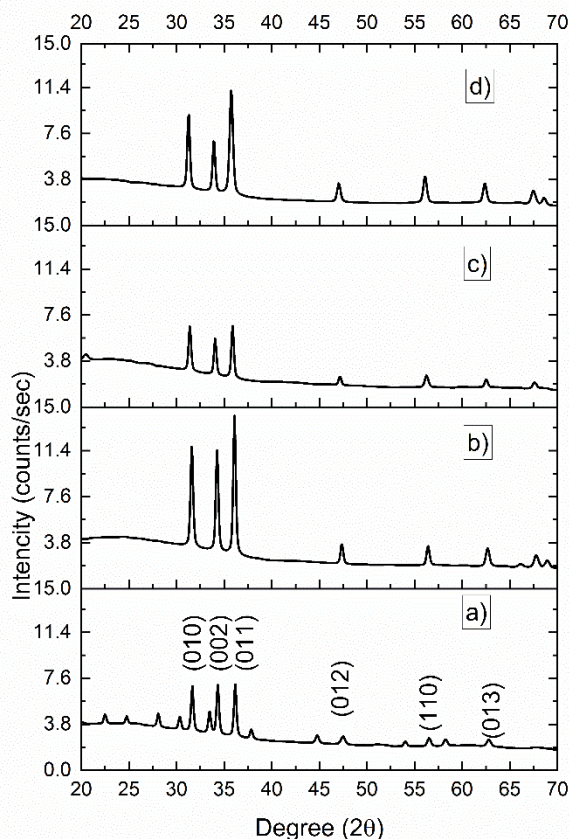


Figure1. Diffraction patterns of XRD for ZnO obtained using different molarities of inhibitor. a) 0 mM, b) 4 mM, c) 8 mM and d) 16 mM of $\text{Na}_2\text{S}_2\text{O}_3$.

In this equation, $I(hkl)$ is the measured relative intensity of a (hkl) plane and $I_0(hkl)$ is the standard intensity of the (hkl) plane given in ASTM card. Preferred orientation values calculated using Equation 2 are given in Table 2. When Figure 1 and Table 2 are examined together, it can be said that the films obtained in S0, S1 and S2 have (011) preferential orientation. On the other hand, the film obtained S3 exhibits two preferred orientations such as (011) and (002),

The Debye Scherrer formula used to calculate the crystallite size was given in Eq. 3 and the calculated values were presented in Table 3.

$$cs = \frac{0.089 * 180 * \lambda}{314 * \beta \cos \theta_c} \text{ nm}$$

$$\lambda = 1.54056 \text{ \AA} \tag{3}$$

It is denoted by the crystal size cs , the wavelength of X-ray radiation λ , the full width half maximum β , and the maximum center $2\theta_c$ [25]. In Table 3, crystallite sizes are given. It can be understood from Table 3 that the average crystallite sizes range from 255 to 292 nm

Table 2. The crystallite size and energy band gaps of the ZnO films.

Experiments	cs (nm) (010)	cs (nm) (002)	cs (nm) (011)	cs(nm) Average	BandGap (eV)
S0	292	287	288	289	3.89
S1	270	275	280	275	4.22
S2	285	303	288	292	4.24
S3	272	275	220	255	4.13

3.2. Optical Properties of The ZnO films

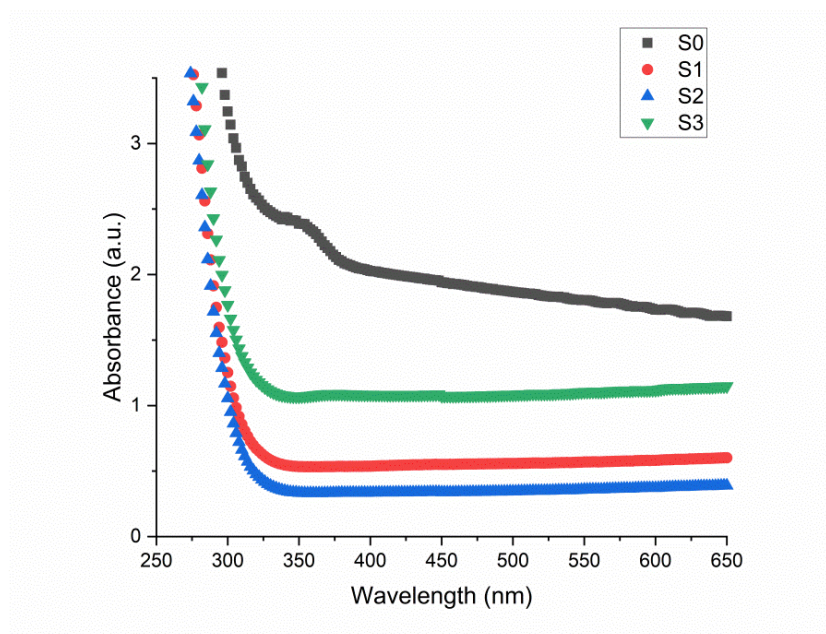


Figure 2. Absorbance measurements of ZnO thin films.

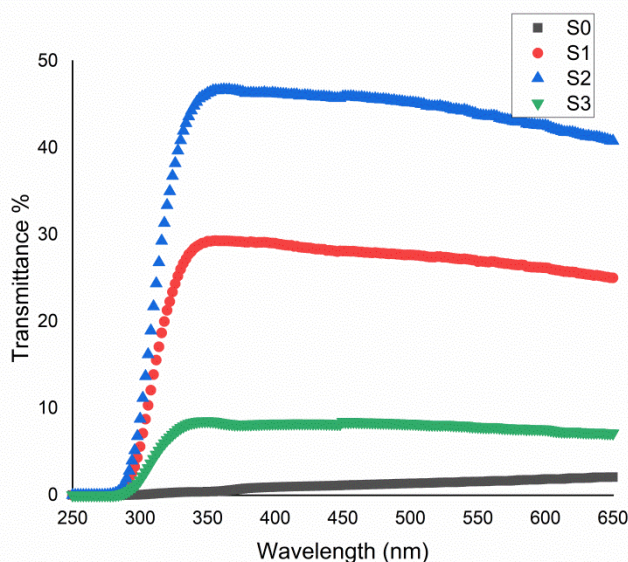


Figure 3. Transmittance plots of ZnO thin films.

Optical absorbance values of ZnO thin films were measured with a UV-Vis spectrometer at wavelengths between 650 and 300 nm and they were shown in Figure 2. Figure 2 shows that the absorbance value of the sample produced without using the inhibitor is 2 to 4 times higher than the samples produced using $\text{Na}_2\text{S}_2\text{O}_3$. This means that the transmittance values of the samples named S1 and S2 increase. Low absorbance and therefore high transmittance values are preferred for window layers of solar cells. Transmittance graphs were given in Figure 3.

The Tauc equation is used to calculate the optical energy band gap of thin films and is shown in Eq. 4.

$$(\alpha h\nu)^2 = A(h\nu - E_g)^n \quad (4)$$

In this equation, α is the absorption coefficient, $h\nu$ is the photon energy, A is the constant, and E_g is the energy band gap of the films. In direct band gap semiconductors, n is $1/2$, in indirect band gap semiconductors it is 2 [26, 27]. ZnO is a direct band gap semiconductor [28]. E_g band gap value is obtained from the $(\alpha h\nu)^2 \sim h\nu$ graph. The point where the line drawn from the upper part of the curve formed in this graph to the $h\nu$ axis intersects the axis gives the band gap value [29]. The energy band gap of thin films is given in Figure 4. Figure 4 shows that the energy band gaps of the films vary between 3.89 eV and 4.24 eV. It is thought that these values may be due to film thicknesses, crystal sizes and surface roughness. It has been observed in the literature that the energy band gaps of ZnO thin films are 3.37 eV [3].

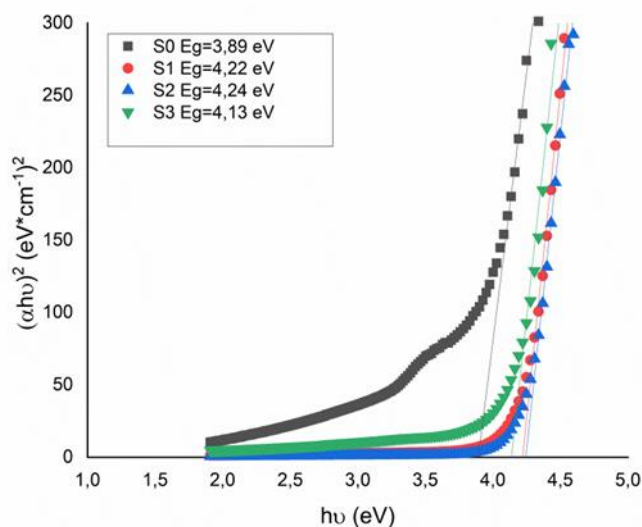


Figure 3. Energy band gaps and Tauc plots of ZnO thin films.

3.3. SEM Analysis of The ZnO films

Scanning electron microscope was used to examine the surface morphology of the produced ZnO thin film samples. Surface images of ZnO films magnified 1000 times and 20000 times were given in Figure 5 and Figure 6 respectively.

In both magnifications, it was observed that nano flowers did not form on the surface of the sample labeled S0, but the entire surface was completely covered. When the surfaces of the samples named S1, S2, and S3 were examined, it is seen that nano flowers were seen on all surfaces, but nano flowers decrease due to the increase in the amount of inhibitor used. It is thought that this situation may be due to the decrease in the reaction rate and the prolongation of the precipitation time due to the use of inhibitor. It can be stated that the surface morphology of the films changes significantly depending on the amount of inhibitor used.

Table 3. Surface roughness values changing depending on the amount of Na₂S₂O₃.

Experiments	Na ₂ S ₂ O ₃ (mM)	Ra (nm)	Rq (nm)
S0	0	42	55
S1	4	56	67
S2	8	54	63
S3	16	51	60

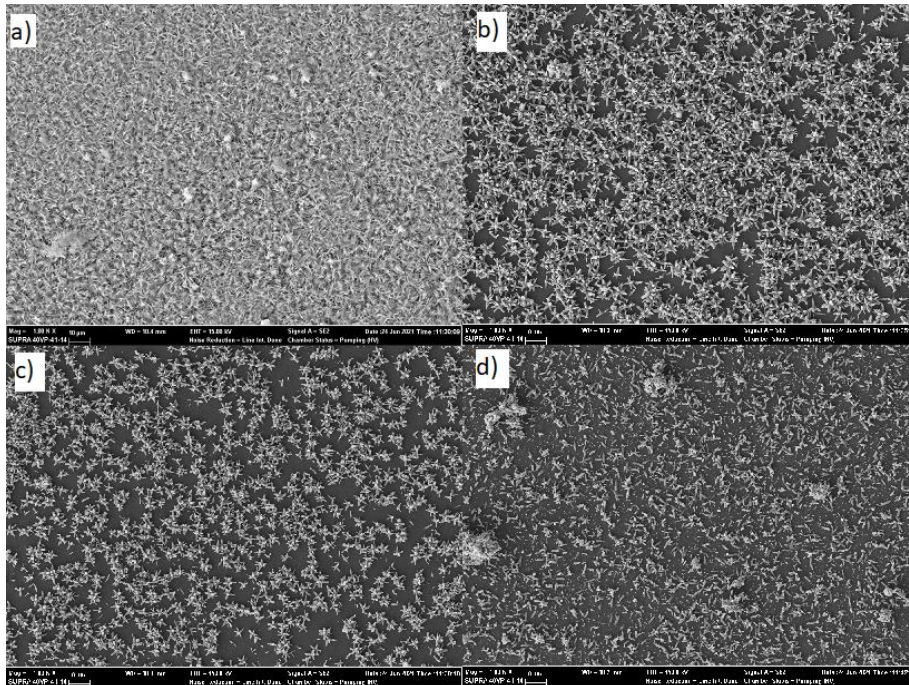


Figure 4. SEM images of ZnO films at 1,000 times magnification.

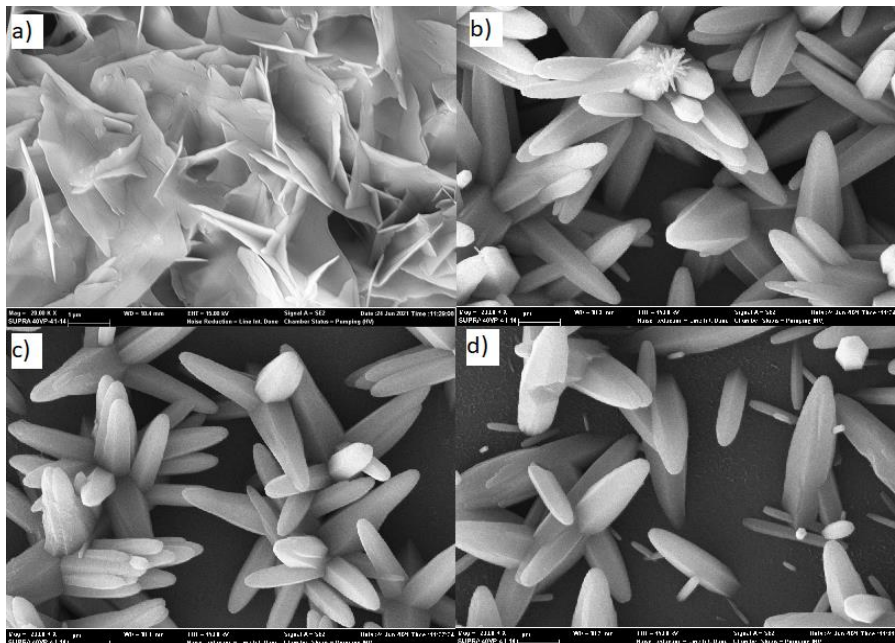


Figure 5. SEM images of ZnO films at 20,000 times magnification.

SEM images used to analyze the surface roughness of the samples were processed with version 1.53c of ImageJ software. The surface roughness images obtained using this software were given in Figure 7 and the calculated average (Ra) and root mean square (Rq) surface roughness values were given in Table 4. When the values given in Table 4 were examined, it was seen that the roughness values of the films produced using inhibitor were relatively high. Due to the high surface roughness values of the films produced using inhibitors, these films are thought to could be a suitable material for gas sensors.

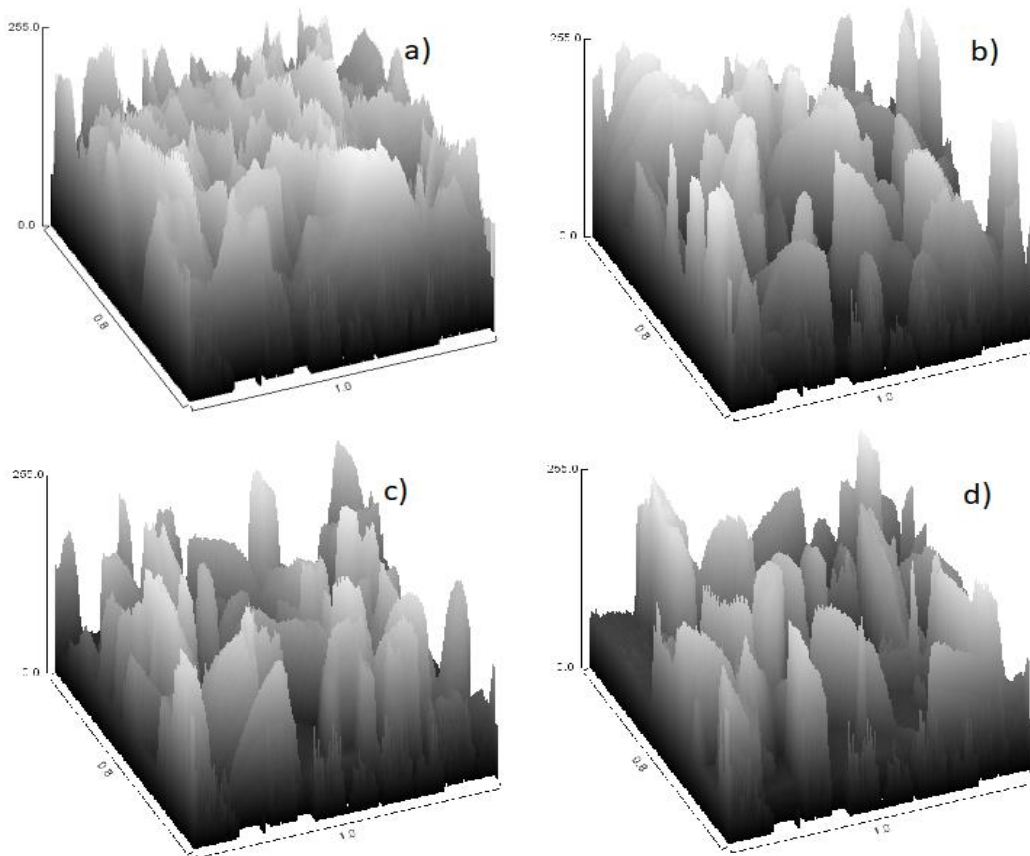


Figure 6. Surface roughness plots of ZnO films.

3.4. Photos of The ZnO Thin Films

Photographs of all ZnO films are shown in Figure 8. All films adhere quite well to the glass substrate surface and the film surfaces appear very compact. However, there was a tonal difference in the image of S0 compared to other films.

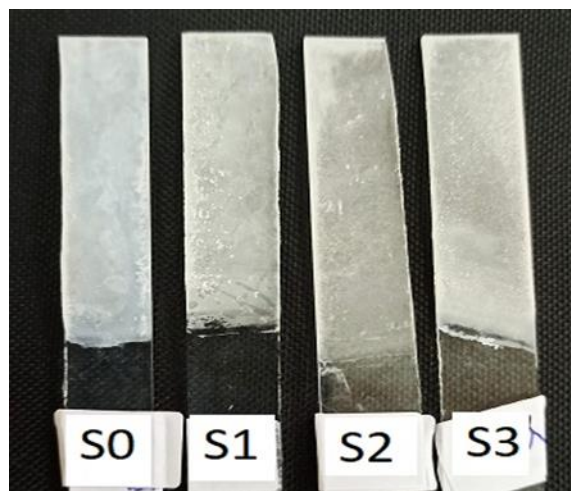


Figure 8. The photographs of the ZnO films.

4. CONCLUSIONS

Thin films of ZnO were precipitated by the chemical bath deposition method and the optical and morphological effects of the amount of $\text{Na}_2\text{S}_2\text{O}_3$ used as an inhibitor on thin films were investigated in this study. Samples were named depending on the amount of inhibitor used. Namely S0- ZnO film produced from the electrolyte without $\text{Na}_2\text{S}_2\text{O}_3$, S1- ZnO film fabricated from the electrolyte with 4 mM $\text{Na}_2\text{S}_2\text{O}_3$, S2- ZnO film deposited from the electrolyte with 8 mM $\text{Na}_2\text{S}_2\text{O}_3$ and S4- ZnO film grown from the electrolyte with 16 mM $\text{Na}_2\text{S}_2\text{O}_3$. Optical analyzes of the films were made, and it was observed that the point where the absorbance increased in the sample named S0 corresponds to a wavelength of 375 nm. It was determined that the absorbance of the other samples increased around 300 nm. At the same time, it was observed that the absorbance values of two samples named S1 and S2 decreased significantly compared to S0 and S3, and the transmittance values increased 20 times. Low absorbance and high transmittance values allow these samples to be utilized as a window layer in thin film solar cells.

The band gap of the samples was calculated using tauc plots. These calculations showed that the energy band gaps of the samples named S0-S1-S2-S3 were 3.89 eV, 4.22 eV, 4.24 eV and 4.13 eV, respectively. According to these results, the use of $\text{Na}_2\text{S}_2\text{O}_3$ as an inhibitor while producing ZnO thin films caused a significant increase in the energy band gaps of the produced thin films.

According to the XRD results, it is seen that all of the films obtained are in hexagonal crystal structure. However, the XRD graph obtained from the sample named S0 shows that there are impurities other than ZnO in the sample. When the XRD graphics of the other samples were examined, it was concluded that the use of $\text{Na}_2\text{S}_2\text{O}_3$ as an inhibitor removed the impurities in the crystal structure.

The surface morphology of the films was examined with a Scanning electron microscope (SEM), SEM images showed that the nano flowers on the film surfaces decreased as the amount of inhibitor

used increased. When the amount of $\text{Na}_2\text{S}_2\text{O}_3$ used was 4 mM and 8 mM, it was observed that the film surfaces were completely covered with nano flowers.

ACKNOWLEDGEMENT

The authors thank the Scientific Research Projects Coordinatorship of Bilecik Şeyh Edebali University for their support for the project titled Production of ZnO Films by Chemical Deposition Method, numbered 2020-02.BŞEÜ.11-01.

REFERENCES

- [1] Temel, S., Gokmen, F. O., and Yaman, E., (2017), Effects of Deposition Time on Structural and Morphological Properties of Synthesized ZnO Nanoflowers Without Using Complexing Agent, *European Scientific Journal, ESJ*, 13(27), 28
- [2] Wang, J. X., Sun, X. W., Yang, Y., Kyaw, K. K. A., Huang, X. Y., Yin, J. Z., ... Demir, H. V., (2011), Free-standing ZnO–CuO composite nanowire array films and their gas sensing properties, *Nanotechnology*, 22(32), 325704.
- [3] Shukla, V., and Patel, A., (2020), Effect of doping concentration on optical and electrical properties of intrinsic n-type ZnO (i-ZnO) and (Cu , Na and K) doped p-type ZnO thin films grown by chemical bath deposition method, *Nanosystems Physics Chemistry Mathematics*, 11(4), 391–400.
- [4] Saraç, U., and Baykul, M. C., (2021), The influence of seed layer electroplating time on structural properties, optical energy bandgap, diameter, growth orientation and surface roughness of ZnO nanorods, *Journal of Materials Science: Materials in Electronics*, 32(22), 26578–26587.
- [5] Wang, H., Liu, Y., Li, M., Huang, H., Xu, H., and Shen, H., (2011), Fabrication of three-dimensional ZnO with hierarchical structure via an electrodeposition process, *Applied Physics A*, 25, 463–466.
- [6] Edinger, S., (2017), Comparison of chemical bath-deposited ZnO films doped with Al , Ga and In, *Journal of Materials Science*, 52(16), 9410–9423.
- [7] Of, O., (2013), Structural Properties of ZnO Thin Films Obtained by Chemical Bath Deposition Technique, *Journal of Nano- and Electronic Physics*, 5(1), 4–7.
- [8] Önal, M., and Altıokka, B., (2020), Effect of stirring on chemically deposited ZnO thin films, *Acta Physica Polonica A*, 137(6), 1209–1213.
- [9] Kumar, S., Kang, H. C. J. T. W., Seth, R., Panwar, S., and Shinde, S. K., (2019), Variation in chemical bath pH and the corresponding precursor concentration for optimizing the optical , structural and morphological properties of ZnO thin films, *Journal of Materials Science: Materials in Electronics*, (0123456789),

- [10] Fortunato, M., Chandraiahgari, C. R., Bellis, G. De, Ballirano, P., Soltani, P., Kaciulis, S., ... Sarto, M. S., (2018), Piezoelectric Thin Films of Grown by Chemical Bath Deposition, *IEEE Transactions on Nanotechnology*, 17(2), 311–319.
- [11] Janotti, A., and Walle, C. G. Van De, (2009), Fundamentals of zinc oxide as a semiconductor, *Reports on progress in physics*, (December),
- [12] I, T. S., and Brien, P. O., (1995), Deposition and characterisation of ZnO thin films grown by chemical bath deposition, *Thin solid films*, 271, 35–38.
- [13] Ramamoorthy, K., Arivanandhan, M., Sankaranarayanan, K., and Sanjeeviraja, C., (2004), Highly textured ZnO thin films : a novel economical preparation and approachment for optical devices , UV lasers and green LEDs, , 85, 257–262.
- [14] Avila-garcı, A., and Ortega-lo, M., (2003), Improved efficiency of the chemical bath deposition method during growth of ZnO thin films, *Materials Research Bulletin*, 38, 1241–1248.
- [15] Masuda, S., Kitamura, K., Okumura, Y., Miyatake, S., Tabata, H., and Kawai, T., (2003), Transparent thin film transistors using ZnO as an active channel layer and their electrical properties, *Journal of Applied Physics*, 93(3), 1624–1630.
- [16] Drici, A., Djeteli, G., Tchangbedji, G., Derouiche, H., Jondo, K., Napo, K., ... Gbagba, M., (2004), Structured ZnO thin films grown by chemical bath deposition for photovoltaic applications, *Physica status solidi (a)*, 1536(7), 1528–1536.
- [17] Ouerfelli, J., Regragui, M., Morsli, M., Djeteli, G., and Jondo, K., (1954), Properties of ZnO thin films deposited by chemical bath deposition and post, *Journal of Physics D: Applied Physics*, 1954.
- [18] Bundesanstalt, P. T., (2008), Electrodeposition of ZnO nanorods for device, *Applied Physics A*, 599(3), 595–599.
- [19] Yuan, Z., (2015), Low-Temperature Growth of Well-Aligned ZnO Nanorod Arrays by Chemical Bath Deposition for Schottky Diode Application, *Journal of Electronic Materials*, 44(4), 1187–1191.
- [20] Önal, M., and Altuokka, B., (2020), Optimization of EDTA – Ammonia Ratio for Chemically Deposited Layers of ZnO Nanoparticles, *Crystallography Reports*, 65(7), 1237–1241.
- [21] Yildizay, H., (2022), Effects of inhibitor on chemically deposited ZnO thin films, *Emerging Materials Research*, Volume 11(1),
- [22] Mohammed, I. M. S., Gubari, G. M. M., Sonawane, M. E., Kasar, R. R., Patil, S. A., Mishra, M. K., ... Sharma, R., (2021), Influence of pH on the physical properties of CdS thin film and its photosensor application, *Applied Physics A: Materials Science and Processing*, 127(8), 1–10.

- [23] Jambure, S. B., Patil, S. J., Deshpande, A. R., and Lokhande, C. D., (2014), A comparative study of physico-chemical properties of CBD and SILAR grown ZnO thin films, *Materials Research Bulletin*, 49(1), 420–425.
- [24] Shaikh, S. K., Inamdar, S. I., Ganbavle, V. V., and Rajpure, K. Y., (2016), Chemical bath deposited ZnO thin film based UV photoconductive detector, *Journal of Alloys and Compounds*, 664, 242–249.
- [25] Bhowmik, R., Murty, M. N., and Srinadhu, E. S., (2008), Magnetic modulation in mechanical alloyed Cr_{1.4}Fe_{0.6}O₃oxide, *PMC Physics B*, 1(1),
- [26] Rahul, Verma, A. K., Tripathi, R. S. N., and Vishwakarma, S. R., (2012), Electrical and optical characterization of electron beam evaporated indium antimonide thin films, *National Academy Science Letters*, 35(5), 367–372.
- [27] Bal, I., Baykul, M. C., and Saraç, U., (2021), The effect of solution temperature on chemically manufactured cds samples, *Chalcogenide Letters*, 18(1), 1–10.
- [28] Berruet, M., and Va, M., (2010), *Materials Science in Semiconductor Processing* Electrodeposition of single and duplex layers of ZnO with different morphologies and electrical properties, *Materials science in semiconductor processing*, 13, 239–244.
- [29] Khan, Z. R., Khan, M. S., Zulfequar, M., and Shahid Khan, M., (2011), Optical and Structural Properties of ZnO Thin Films Fabricated by Sol-Gel Method, *Materials Sciences and Applications*, 02(05), 340–345.